# Evidence Against a Dark Matter Explanation of the Fermi GeV excess

arXiv:1611.06644

*Image credit:ESO*

Oscar Macias

TeVPA 2017

OSU, August 7 – 11, 2017

VirginiaTech
Invent the Future®

# The Fermi-LAT GeV gamma-ray excess

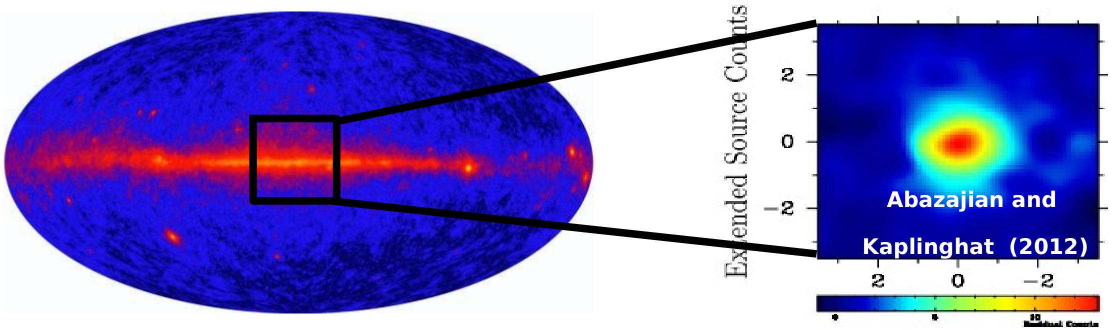


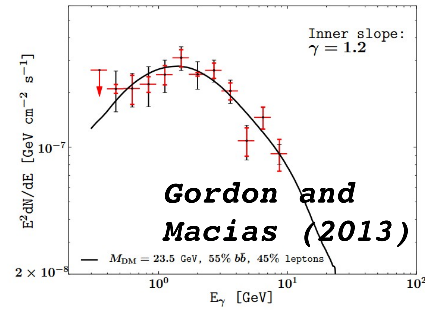


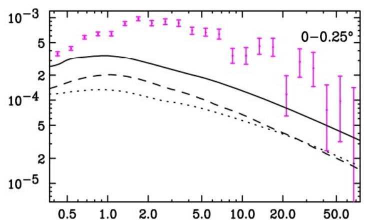


Goodenough and Hooper (2009)

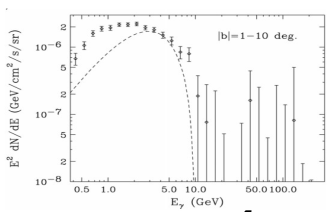


Hooper and Slatyer (2013)

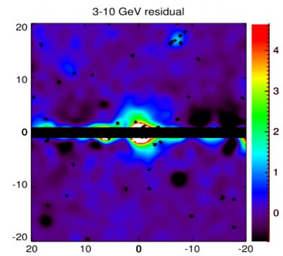


Daylan et al.(2016)

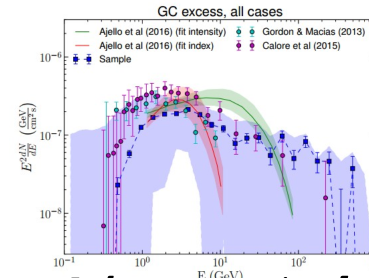


Ackermann et al.(2017)

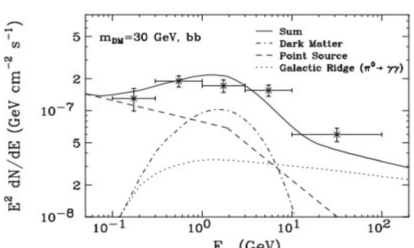


Hooper and Linden (2011)

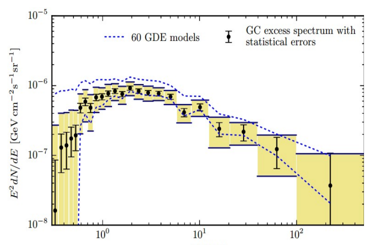


Calore et al. (2015)

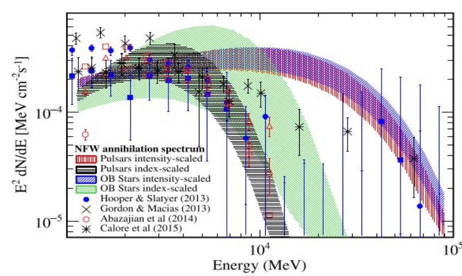


Ajello et al. (2016)

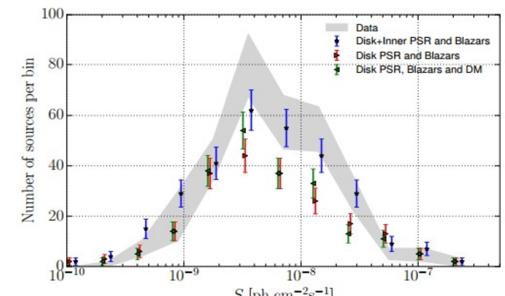


Ajello et al.(2017)

**Many studies have found the GeV excess is best-fit by an NFW density profile. Here we do a reanalysis of the spatial morphology of the GeV excess.**

# Analysis Set-up

## 1) Data set used in this analysis:

- ~7 years of Pass8 UltraCleanVeto class
- E = 667 MeV – 158 GeV
- ROI = 15x15 deg region around the GC

## 2) Fitting Technique:

- Spectrum: Bin-by-bin analysis
- Spatial morphology: Template fitting method

## 3) Analysis Methods:

- Use alternative interstellar gas maps
  - Interpolated and hydrodynamical gas maps
- What is the GeV excess associated with?
  - Bulge stellar distributions, new point sources, Fermi Bubbles, Dark Matter?

# The Base Model

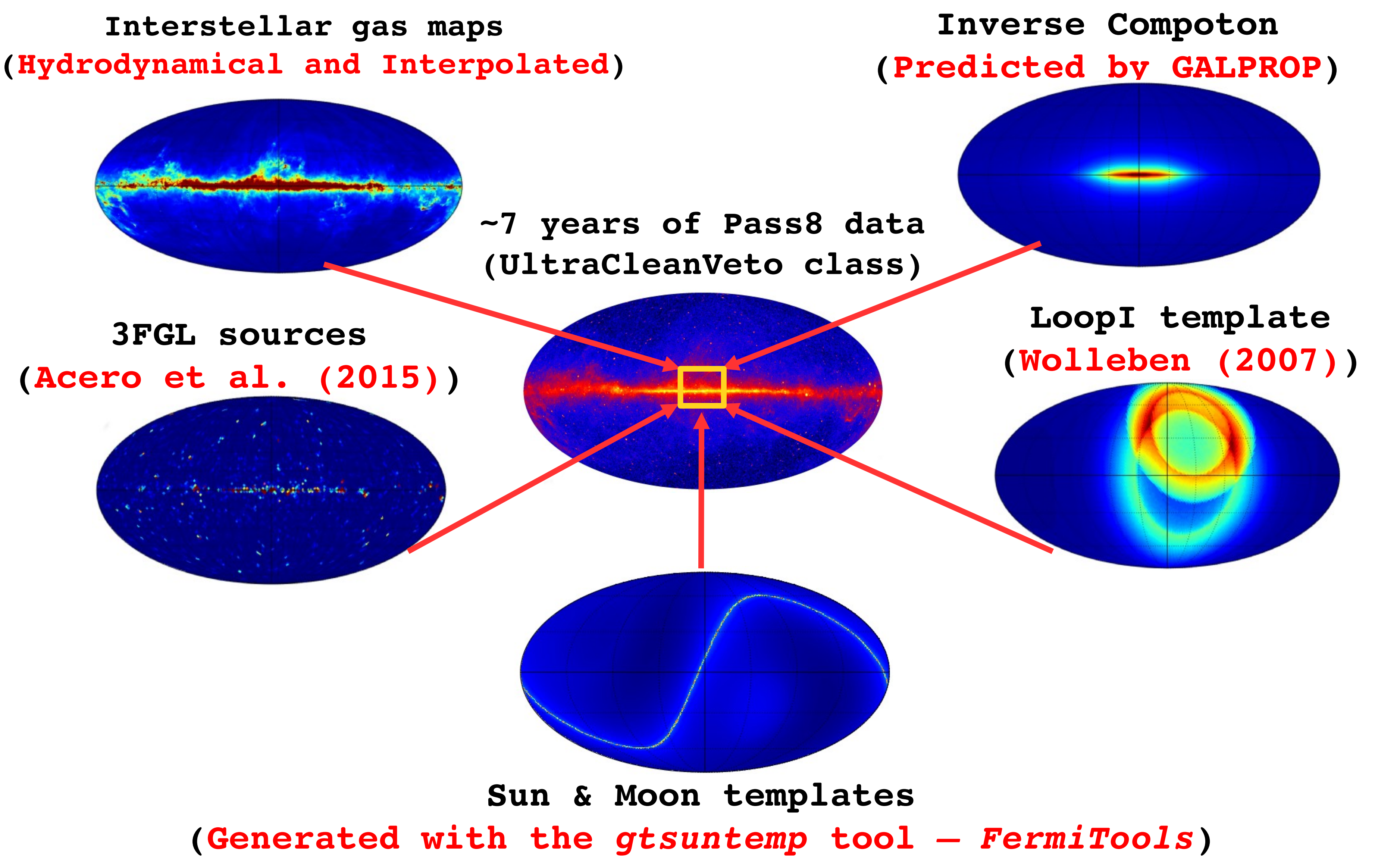

# Interpolated vs Hydrodynamical method

*Macias et al. (2016)*

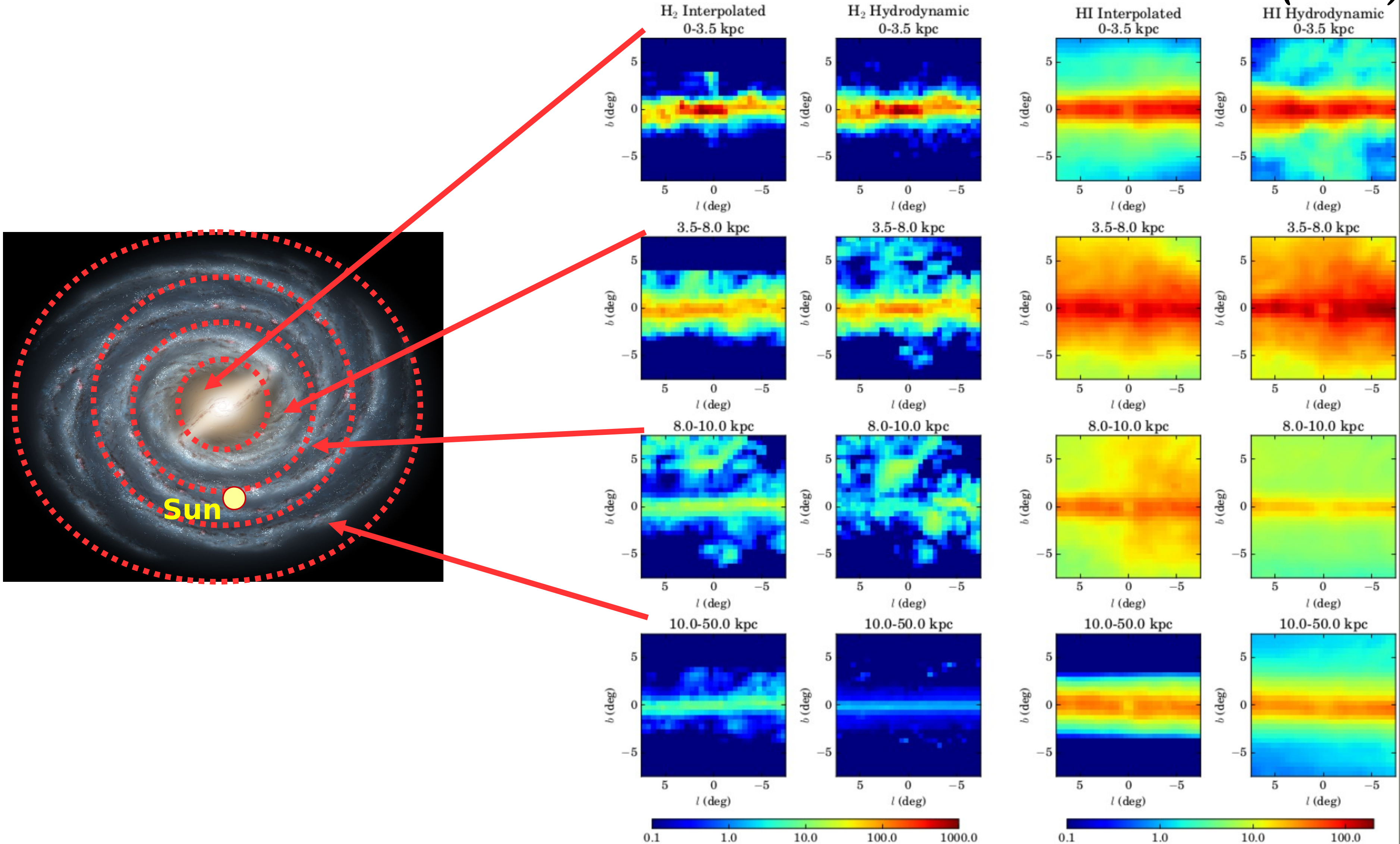


**There are noticeable morphological differences between the two methods.**

# Hydrodynamical vs Interpolated maps

*Macias et al. (2016)*

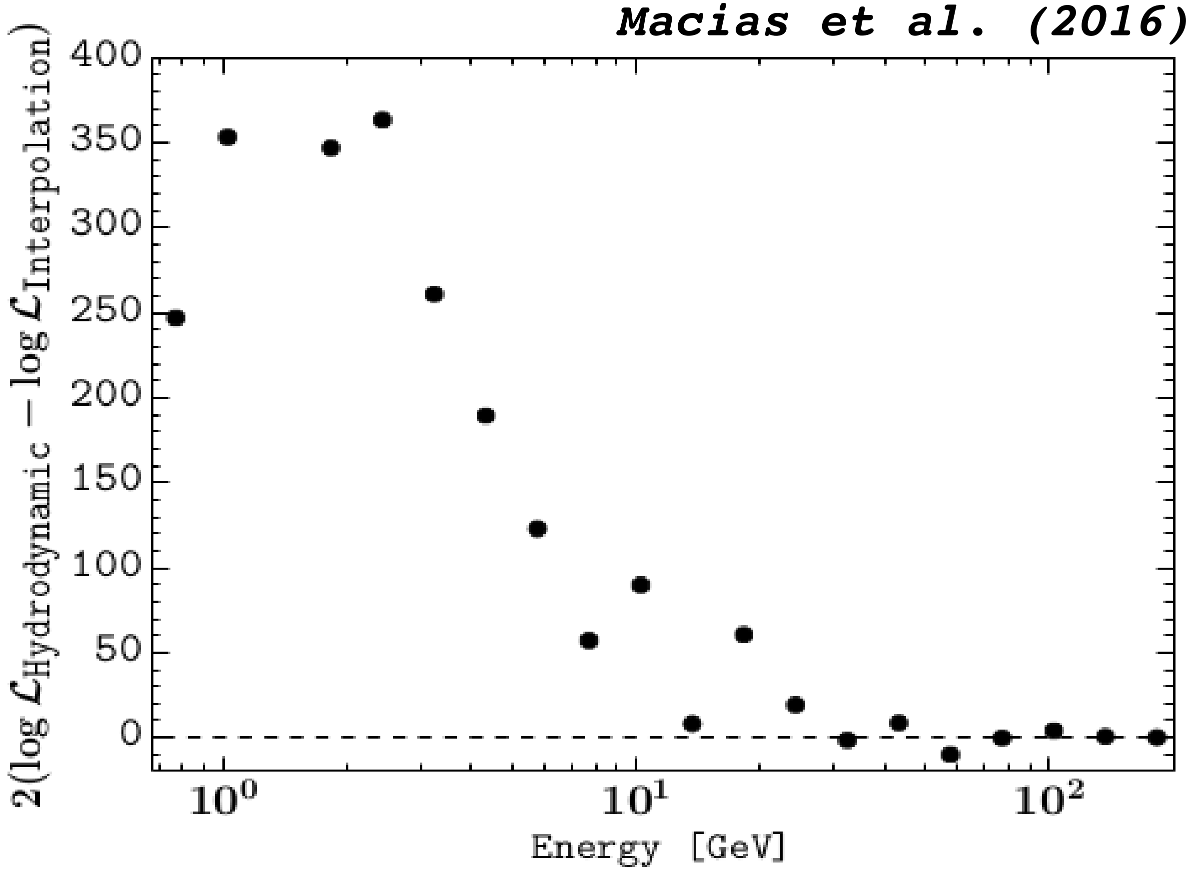


The **hydrodynamical gas maps are preferred** by the data at almost every energy bin.

# New point source candidates in the ROI

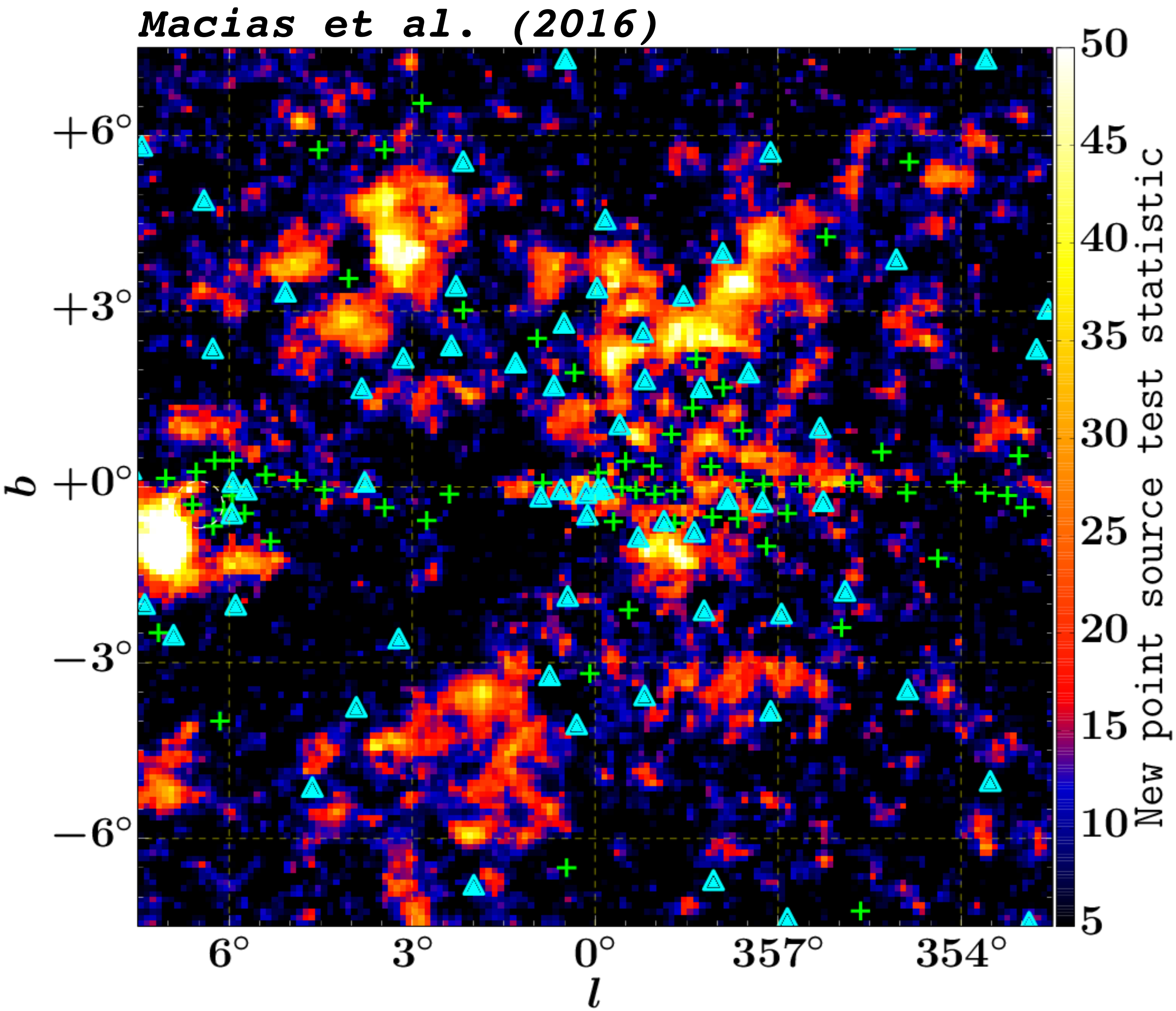


**Detection threshold:**
**TS > 41.8**
**(for 19 d.o.f.)**

**Found 64 gamma-ray point source candidates in the inner 15x15 deg RoI of the Galactic Center**

# Comparison with new point sources in 2FIG

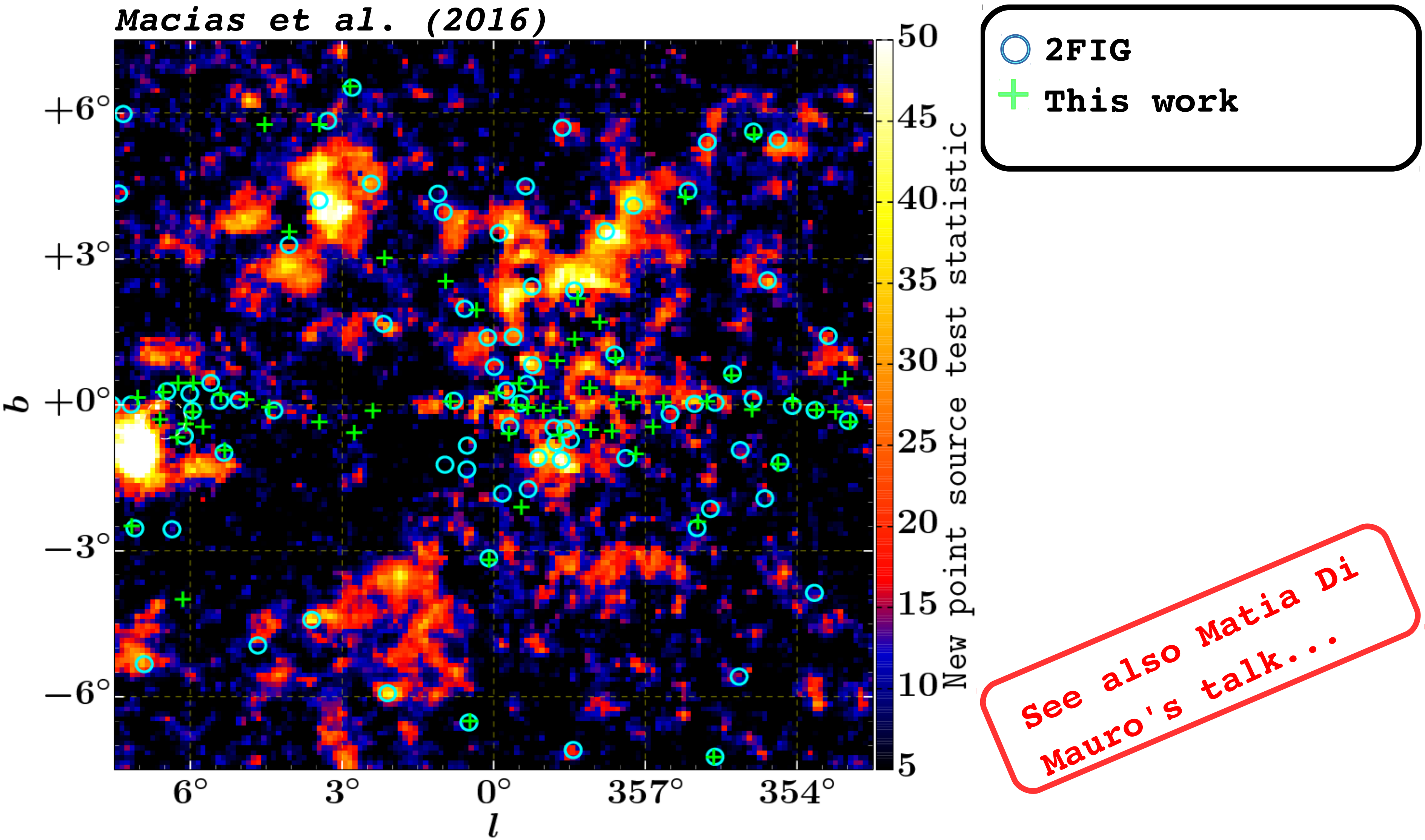


See also Matia Di Mauro's talk...

There are 81 new point sources in 2FIG and 64 in our work. Our analysis confirms 31 2FIG PSs.

# Residual extended gamma-rays

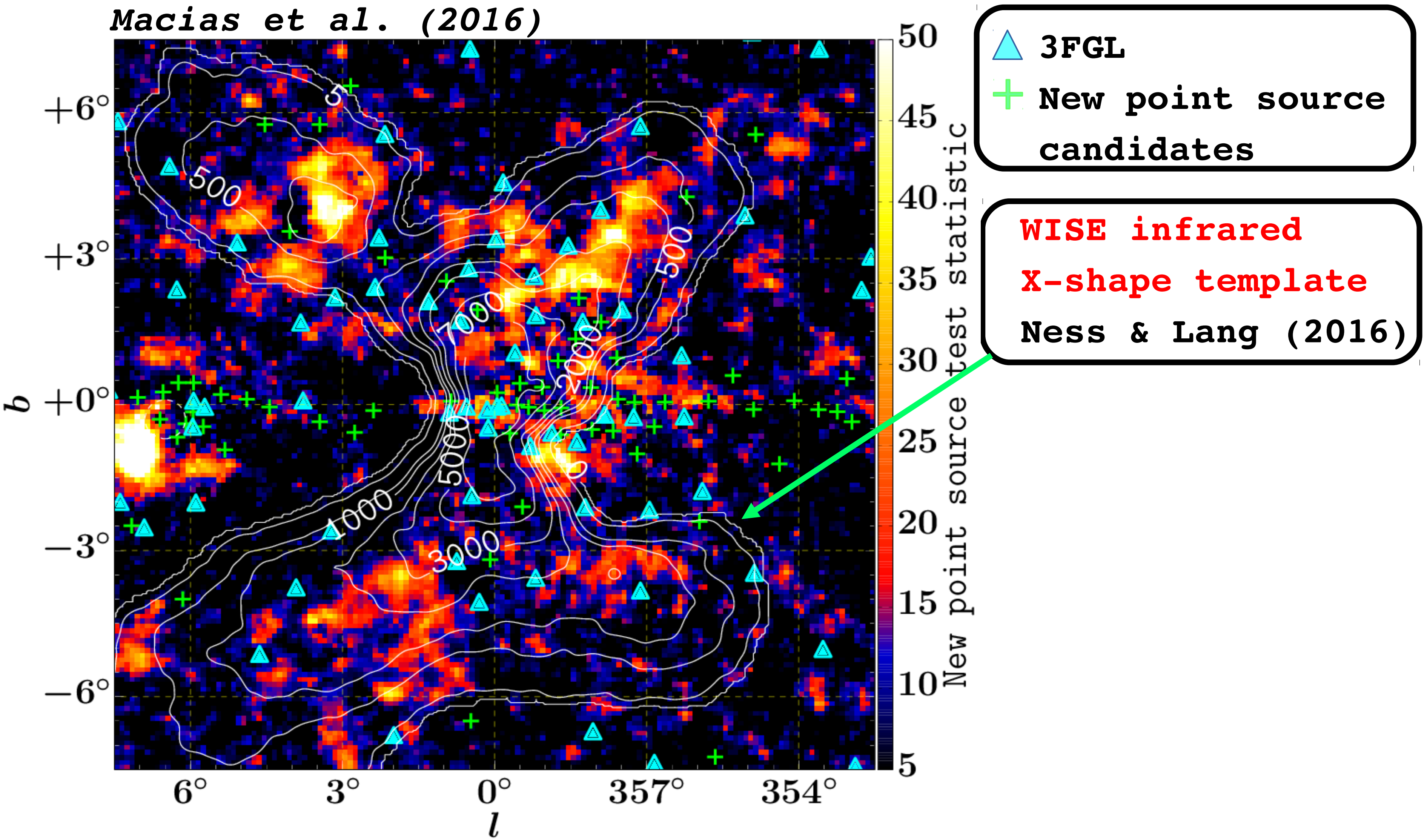


There is residual extended emission which looks very similar to the X-shaped infrared bulge.

# The X-shaped/Boxy Galactic Bulge


Close to 33% of all Galaxies display a boxy/penaut or X-shaped bulge when seen edge on [Jarvis 1986].

# The X-shaped/Boxy Galactic Bulge


Close to 33% of all Galaxies display a boxy/penaut or X-shaped bulge when seen edge on [Jarvis 1986].

# The X-shaped/Boxy Galactic Bulge


***The Boxy Bulge***

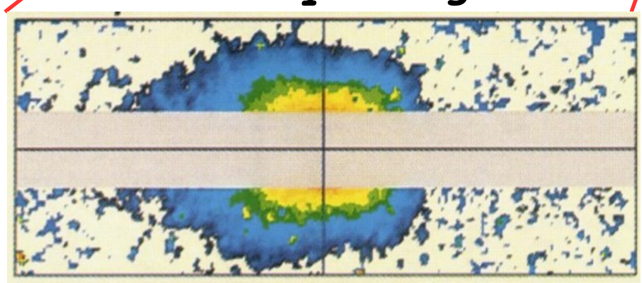

*Weiland et al. (1994)*
*(COBE diffuse Infrared emission)*

**See also Richard Bartel's talk...**

**COBE observations of the Galactic bulge reveal a boxy shape morphology.**

# The X-shaped/Boxy Galactic Bulge


The Boxy Bulge

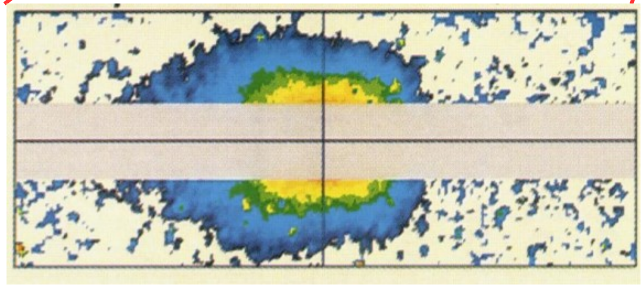

Weiland et al. (1994)
(DIRBE observatory on board of the COBE satellite )

Improved resolution with the WISE telescope

The X-shaped Bulge

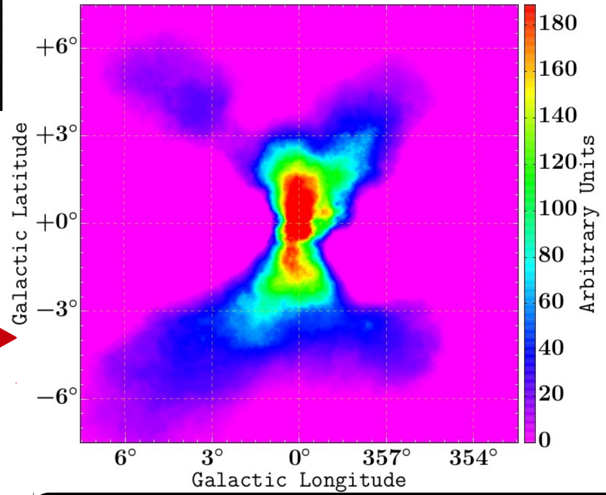


Ness and Lang (2016)
(WISE diffuse Infrared emission)

More precise WISE observations of the Galactic bulge reveal an X-shaped bulge morphology.

# The X-shaped Bulge and the Nuclear Bulge


***The X-shaped Bulge***

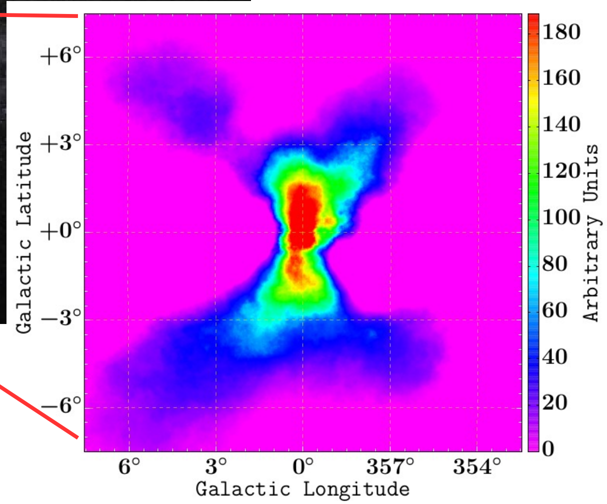


***Ness and Lang (2016)***
***(WISE diffuse Infrared emission)***

***The Nuclear Bulge***

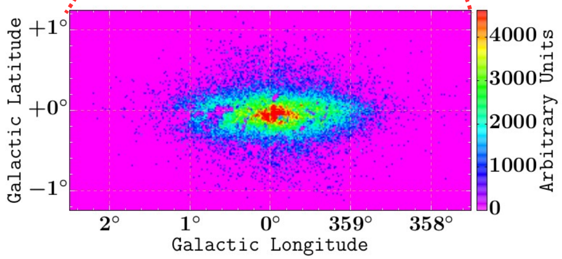


***Nishiyama et al. (2013)***
***(Stellar count map in the inner 230 pc)***

**There is an additional dense and disky stellar population close to the supermassive black hole.**

# Main Results

| Base | Source | $\log(\mathcal{L}_{\rm Base})$ | $\log(\mathcal{L}_{\rm Base+Source})$ | $\rm TS_{Source}$ | $\sigma$ | Number of source parameters |
|---|---|---|---|---|---|---|
| baseline | FB | -172461.4 | -172422.3 | 78 | 6.9 | 19 |
| baseline | NFW-s | -172461.4 | -172265.3 | 392 | 18.4 | 19 |
| baseline | X-bulge | -172461.4 | -172224.1 | 475 | 20.5 | 19 |
| baseline | NFW | -172461.4 | -172167.9 | 587 | 23.0 | 19 |
| baseline | NB | -172461.4 | -171991.8 | 939 | 29.5 | 19 |
| baseline | NP | -172461.4 | -169804.1 | 5315 | 55.7 | $64 \times 19$ |
| baseline+NP | FB | -169804.1 | -169773.6 | 61 | 5.8 | 19 |
| baseline+NP | NB | -169804.1 | -169697.2 | 214 | 13.0 | 19 |
| baseline+NP | NFW | -169804.1 | -169623.3 | 362 | 17.6 | 19 |
| baseline+NP | X-bulge | -169804.1 | -169616.2 | 376 | 18.0 | 19 |
| baseline+NP+X-bulge | NFW | -169616.2 | -169568.4 | 96 | 7.9 | 19 |
| baseline+NP+X-bulge | NB | -169616.2 | -169542.0 | 148 | 10.4 | 19 |
| baseline+NP+X-bulge+NB | NFW | -169542.0 | -169531.0 | 22 | 2.4 | 19 |
| baseline+NP+X-bulge+NB | FB | -169542.0 | -169525.5 | 33 | 3.5 | 19 |
| baseline+NP+NB | X-bulge | -169697.2 | -169542.0 | 310 | 16.1 | 19 |
| baseline+NP+NFW | X-bulge+NB | -169623.3 | -169531.0 | 185 | 10.8 | $2 \times 19$ |

**NP:=New point sources**
**NB:=Nuclear Bulge**
**FB:=Fermi Bubbles**

*To appear in a new version of Macias et al. (2016)*

# Main Results

| Base | Source | $\log(\mathcal{L}_{\rm Base})$ | $\log(\mathcal{L}_{\rm Base+Source})$ | $\rm TS_{Source}$ | $\sigma$ | Number of source parameters |
|---|---|---|---|---|---|---|
| baseline | FB | -172461.4 | -172422.3 | 78 | 6.9 | 19 |
| baseline | NFW-s | -172461.4 | -172265.3 | 392 | 18.4 | 19 |
| baseline | X-bulge | -172461.4 | -172224.1 | 475 | 20.5 | 19 |
| baseline | NFW | -172461.4 | -172167.9 | 587 | 23.0 | 19 |
| baseline | NB | -172461.4 | -171991.8 | 939 | 29.5 | 19 |
| baseline | NP | -172461.4 | -169804.1 | 5315 | 55.7 | $64 \times 19$ |
| baseline+NP | FB | -169804.1 | -169773.6 | 61 | 5.8 | 19 |
| baseline+NP | NB | -169804.1 | -169697.2 | 214 | 13.0 | 19 |
| baseline+NP | NFW | -169804.1 | -169623.3 | 362 | 17.6 | 19 |
| baseline+NP | X-bulge | -169804.1 | -169616.2 | 376 | 18.0 | 19 |
| baseline+NP+X-bulge | NFW | -169616.2 | -169568.4 | 96 | 7.9 | 19 |
| baseline+NP+X-bulge | NB | -169616.2 | -169542.0 | 148 | 10.4 | 19 |
| baseline+NP+X-bulge+NB | NFW | -169542.0 | -169531.0 | 22 | 2.4 | 19 |
| baseline+NP+X-bulge+NB | FB | -169542.0 | -169525.5 | 33 | 3.5 | 19 |
| baseline+NP+NB | X-bulge | -169697.2 | -169542.0 | 310 | 16.1 | 19 |
| baseline+NP+NFW | X-bulge+NB | -169623.3 | -169531.0 | 185 | 10.8 | $2 \times 19$ |

***To appear in a new version of Macias et al. (2016)***

**NP:=New point sources**

**NB:=Nuclear Bulge**

**FB:=Fermi Bubbles**

# Main Results

| Base | Source | $\log(\mathcal{L}_{\text{Base}})$ | $\log(\mathcal{L}_{\text{Base+Source}})$ | $\text{TS}_{\text{Source}}$ | $\sigma$ | Number of source parameters |
|---|---|---|---|---|---|---|
| baseline | FB | -172461.4 | -172422.3 | 78 | 6.9 | 19 |
| baseline | NFW-s | -172461.4 | -172265.3 | 392 | 18.4 | 19 |
| baseline | X-bulge | -172461.4 | -172224.1 | 475 | 20.5 | 19 |
| baseline | NFW | -172461.4 | -172167.9 | 587 | 23.0 | 19 |
| baseline | NB | -172461.4 | -171991.8 | 939 | 29.5 | 19 |
| baseline | NP | -172461.4 | -169804.1 | 5315 | 55.7 | $64 \times 19$ |
| baseline+NP | FB | -169804.1 | -169773.6 | 61 | 5.8 | 19 |
| baseline+NP | NB | -169804.1 | -169697.2 | 214 | 13.0 | 19 |
| baseline+NP | NFW | -169804.1 | -169623.3 | 362 | 17.6 | 19 |
| baseline+NP | X-bulge | -169804.1 | -169616.2 | 376 | 18.0 | 19 |
| baseline+NP+X-bulge | NFW | -169616.2 | -169568.4 | 96 | 7.9 | 19 |
| baseline+NP+X-bulge | NB | -169616.2 | -169542.0 | 148 | 10.4 | 19 |
| baseline+NP+X-bulge+NB | NFW | -169542.0 | -169531.0 | 22 | 2.4 | 19 |
| baseline+NP+X-bulge+NB | FB | -169542.0 | -169525.5 | 33 | 3.5 | 19 |
| baseline+NP+NB | X-bulge | -169697.2 | -169542.0 | 310 | 16.1 | 19 |
| baseline+NP+NFW | X-bulge+NB | -169623.3 | -169531.0 | 185 | 10.8 | $2 \times 19$ |

*To appear in a new version of Macias et al. (2016)*

**NP:=New point sources**
**NB:=Nuclear Bulge**
**FB:=Fermi Bubbles**

# Main Results

| Base | Source | $\log(\mathcal{L}_{\text{Base}})$ | $\log(\mathcal{L}_{\text{Base+Source}})$ | $TS_{\text{Source}}$ | $\sigma$ | Number of source parameters |
|---|---|---|---|---|---|---|
| baseline | FB | -172461.4 | -172422.3 | 78 | 6.9 | 19 |
| baseline | NFW-s | -172461.4 | -172265.3 | 392 | 18.4 | 19 |
| baseline | X-bulge | -172461.4 | -172224.1 | 475 | 20.5 | 19 |
| baseline | NFW | -172461.4 | -172167.9 | 587 | 23.0 | 19 |
| baseline | NB | -172461.4 | -171991.8 | 939 | 29.5 | 19 |
| baseline | NP | -172461.4 | -169804.1 | 5315 | 55.7 | $64 \times 19$ |
| baseline+NP | FB | -169804.1 | -169773.6 | 61 | 5.8 | 19 |
| baseline+NP | NB | -169804.1 | -169697.2 | 214 | 13.0 | 19 |
| baseline+NP | NFW | -169804.1 | -169623.3 | 362 | 17.6 | 19 |
| baseline+NP | X-bulge | -169804.1 | -169616.2 | 376 | 18.0 | 19 |
| baseline+NP+X-bulge | NFW | -169616.2 | -169568.4 | 96 | 7.9 | 19 |
| baseline+NP+X-bulge | NB | -169616.2 | -169542.0 | 148 | 10.4 | 19 |
| baseline+NP+X-bulge+NB | NFW | -169542.0 | -169531.0 | 22 | 2.4 | 19 |
| baseline+NP+X-bulge+NB | FB | -169542.0 | -169525.5 | 33 | 3.5 | 19 |
| baseline+NP+NB | X-bulge | -169697.2 | -169542.0 | 310 | 16.1 | 19 |
| baseline+NP+NFW | X-bulge+NB | -169623.3 | -169531.0 | 185 | 10.8 | $2 \times 19$ |

*To appear in a new version of Macias et al. (2016)*

**NP:=New point sources**
**NB:=Nuclear Bulge**
**FB:=Fermi Bubbles**

# Main Results

| Base | Source | $\log(\mathcal{L}_{\text{Base}})$ | $\log(\mathcal{L}_{\text{Base+Source}})$ | $\text{TS}_{\text{Source}}$ | $\sigma$ | Number of source parameters |
|---|---|---|---|---|---|---|
| baseline | FB | -172461.4 | -172422.3 | 78 | 6.9 | 19 |
| baseline | NFW-s | -172461.4 | -172265.3 | 392 | 18.4 | 19 |
| baseline | X-bulge | -172461.4 | -172224.1 | 475 | 20.5 | 19 |
| baseline | NFW | -172461.4 | -172167.9 | 587 | 23.0 | 19 |
| baseline | NB | -172461.4 | -171991.8 | 939 | 29.5 | 19 |
| baseline | NP | -172461.4 | -169804.1 | 5315 | 55.7 | $64 \times 19$ |
| baseline+NP | FB | -169804.1 | -169773.6 | 61 | 5.8 | 19 |
| baseline+NP | NB | -169804.1 | -169697.2 | 214 | 13.0 | 19 |
| baseline+NP | NFW | -169804.1 | -169623.3 | 362 | 17.6 | 19 |
| baseline+NP | X-bulge | -169804.1 | -169616.2 | 376 | 18.0 | 19 |
| baseline+NP+X-bulge | NFW | -169616.2 | -169568.4 | 96 | 7.9 | 19 |
| baseline+NP+X-bulge | NB | -169616.2 | -169542.0 | 148 | 10.4 | 19 |
| baseline+NP+X-bulge+NB | NFW | -169542.0 | -169531.0 | 22 | 2.4 | 19 |
| baseline+NP+X-bulge+NB | FB | -169542.0 | -169525.5 | 33 | 3.5 | 19 |
| baseline+NP+NB | X-bulge | -169697.2 | -169542.0 | 310 | 16.1 | 19 |
| baseline+NP+NFW | X-bulge+NB | -169623.3 | -169531.0 | 185 | 10.8 | $2 \times 19$ |

*To appear in a new version of Macias et al. (2016)*

**NP:=New point sources**
**NB:=Nueclear Bulge**
**FB:=Fermi Bubbles**

**The Fermi GeV excess is best-fit by the X-bulge + Nuclear Bulge. The NFW template does not improve the fit and is therefore not required by the data**

# Main Results: Fermi GeV excess spatial Morphology

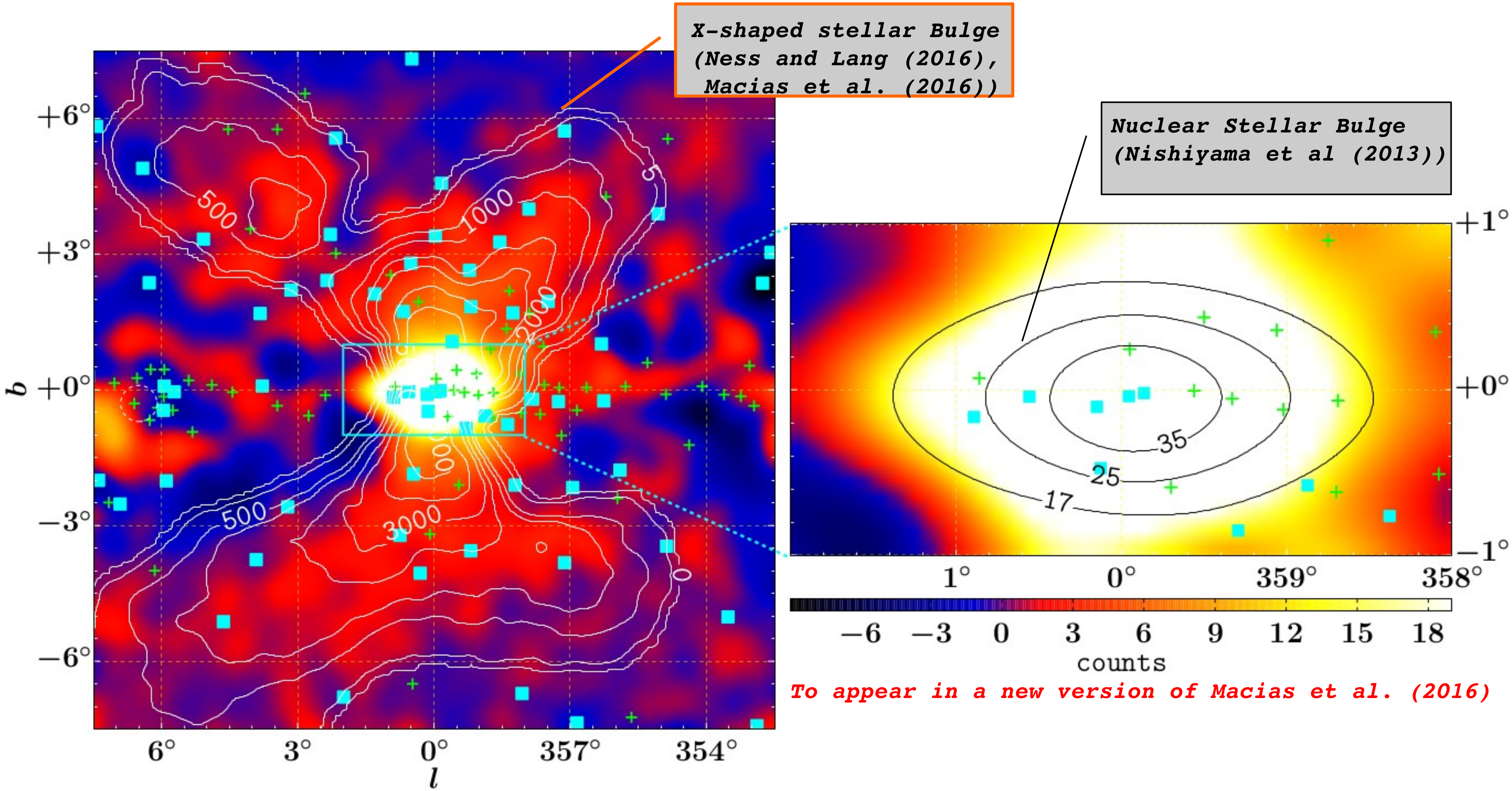


*To appear in a new version of Macias et al. (2016)*

**The Galactic Center excess gamma-rays are distributed as the X-bulge + Nuclear bulge stars.**

# Main Results: Spectrum of X-bulge + Nuclear Bulge

*To appear in a new version of Macias et al. (2016)*

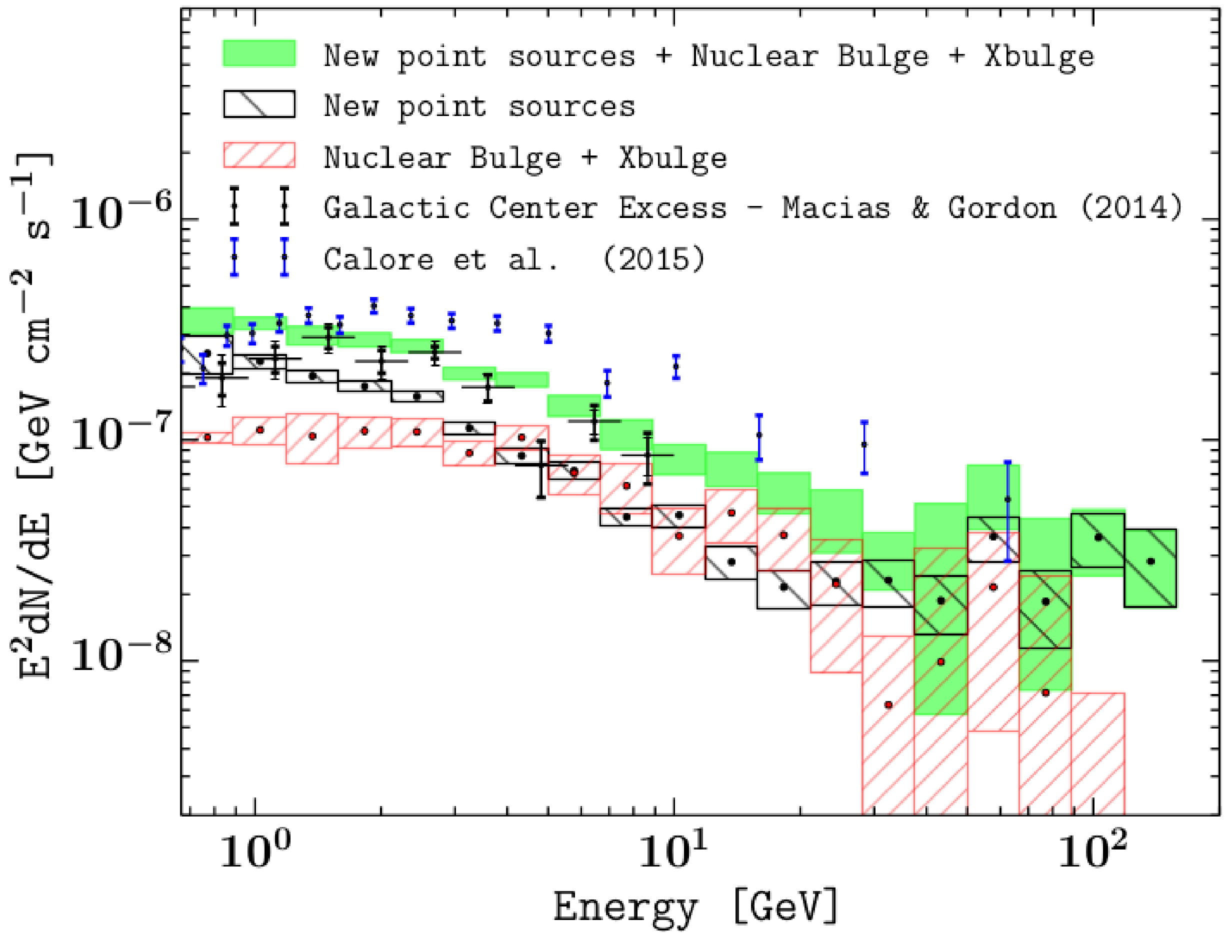


**The spectrum of the X-bulge + Nuclear bulge is consistent with that of MSPs.**

# Conclusions

1) Gas Maps for the Galactic Center

Hydrodynamical gas maps provide a better fit to the data than the interpolated gas maps in the inner 15x15 deg of the GC.

2) What is the Galactic Center excess due to?

Is very plausible that the Fermi GeV excess is associated with stellar bulge populations e.g. MSPs.

Thanks!

# Back up slides

# Summary

- Analyzed Fermi-LAT Galactic center excess emission taking into account degeneracy with point sources and systematics in diffuse Galactic background.
- Interstellar gas maps constructed with the help of hydrodynamical simulations are a better description of the data than the ones constructed with the interpolation approach used in most previous works.
- Found 64 new gamma-ray point source candidates. Confirmed the existence of 31 new point sources in the 2FIG catalog.
- The spatial morphology is Galactic Center excess is spatially distributed as the previously known X-shaped bulge infrared emission and the nuclear bulge stellar population map.
- Found of order 10^4 or unresolved millisecond pulsars in the Xbulge could account for the excess emission.
- Annihilating dark matter is not longer a good fitting model for the Galactic center excess.

# Detection Threshold

***In our bin-by-bin analysis we had 19 energy bands in each of which the point source amplitude was not allowed to take on a negative value, we thus have a mixture distribution given by***

$$p(\mathrm{TS}) = \frac{\delta(\mathrm{TS}) + \sum_{i=1}^{19} \binom{19}{i} \chi^2_{i+2}(\mathrm{TS})}{\sum_{i=0}^{19} \binom{19}{i}}$$

***To work out the number of σ of a detection we evaluate the equivalent p-value for a one new parameter case:***

$$\text{Number of } \sigma \equiv \sqrt{\text{InverseCDF}\left(\chi^2_1, \text{CDF}\left[\text{p(TS)}, \hat{\text{TS}}\right]\right)}$$

***For 19 d.o.f a 4σ detection corresponds to TS>41.8.***

# Analysis of the Systematics

| Base | Source | $\log(\mathcal{L}_{\rm Base})$ | $\log(\mathcal{L}_{\rm Base+Source})$ | $\rm TS_{Source}$ | $\sigma$ | Number of source parameters |
|---|---|---|---|---|---|---|
| baseline+NB+X-bulge | NFW | -171956.4 | -171948.7 | 15 | 1.5 | 19 |
| baseline+NFW | NB+X-bulge | -172167.9 | -171948.7 | 438 | 18.6 | $2 \times 19$ |
| baseline$^\star$ | NFW | -173565.0 | -172929.2 | 1272 | 34.6 | 19 |
| baseline$^\star$+NFW | NB+X-bulge | -172929.2 | -172592.0 | 674 | 23.8 | $2 \times 19$ |
| baseline$^\star$+NB+X-bulge | NFW | -172631.5 | -172592.0 | 79 | 6.9 | 19 |
| baseline | 2FIG | -172461.4 | -170710.5 | 3501 | 37.3 | $81 \times 19$ |
| baseline+2FIG | X-bulge | -170710.5 | -170487.3 | 446 | 19.8 | 19 |
| baseline+2FIG | NFW | -170710.5 | -170484.6 | 452 | 19.9 | 19 |
| baseline+2FIG | NB | -170710.5 | -170470.5 | 480 | 20.6 | 19 |
| baseline+2FIG+NB | NFW | -170470.5 | -170387.8 | 165 | 11.1 | 19 |
| baseline+2FIG+NB | X-bulge | -170470.5 | -170307.6 | 326 | 16.6 | 19 |
| baseline+2FIG+NB+Xbulge | NFW | -170307.6 | -170301.8 | 12 | 1.1 | 19 |

*To appear in a new version of Macias et al. (2016)*

**baseline:= Hydrodynamical gas maps**

**baseline*:= Interpolated gas maps**

**NP:= New point sources**

**NB:= Nuclear Bulge**

**FB:= Fermi Bubbles**

**2FIG:= 81 new point sources in the 15x15 RoI**

# The X-shaped Stellar Population of the Galactic Bulge


*Macias et al. (2016)*
*Ness and Lang (2016)*

**Dynamical instabilities** of stars in the Galactic bar send these on orbits resembling an **X-shape**

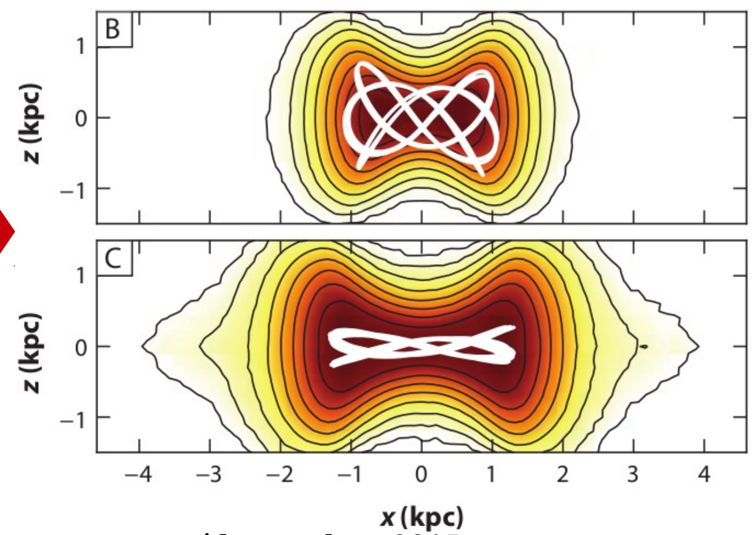


*Portail et al. (2015)*
*Bland-Hawthorn & Gerhard (2016)*

# Xco values at the Galactic Center

*Ackermann et al. (2012)*

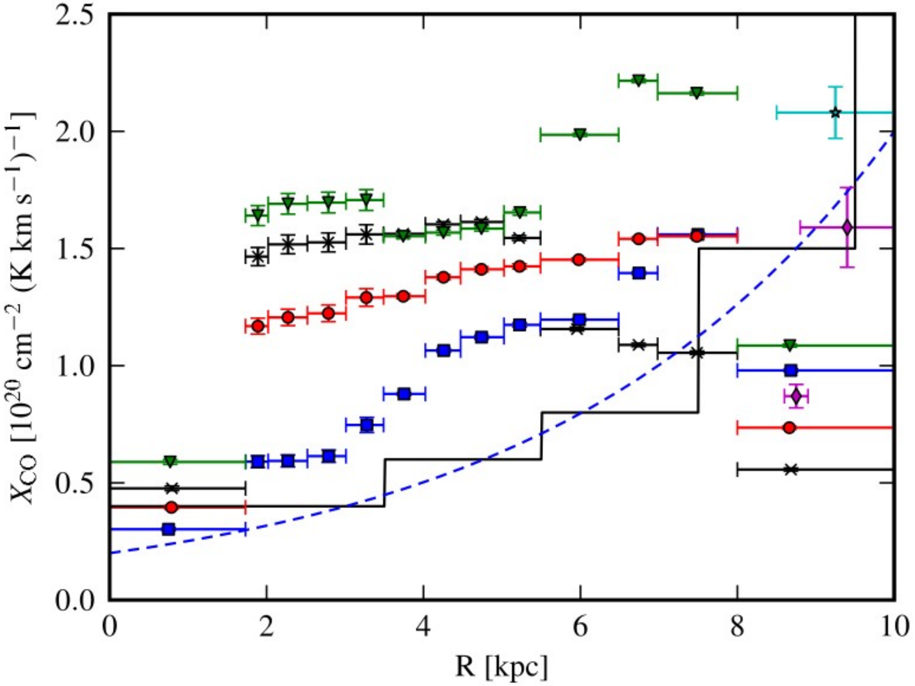


**Radial distribution of Xco at the Galactic Center**

| Annulus | 0 – 3.5 kpc | 3.5 – 8.0 kpc | 8.0 – 10.0 kpc |
|---|---|---|---|
| $X_{CO}$ | $0.4 \pm 0.1$ | $1.1 \pm 0.2$ | $3.6 \pm 1.3$ |

*Macias et al. (2016)*

{ Xco values from our fits are physically plausible.

# Spectrum of best-fitting model components

*Macias et al. (2016)*

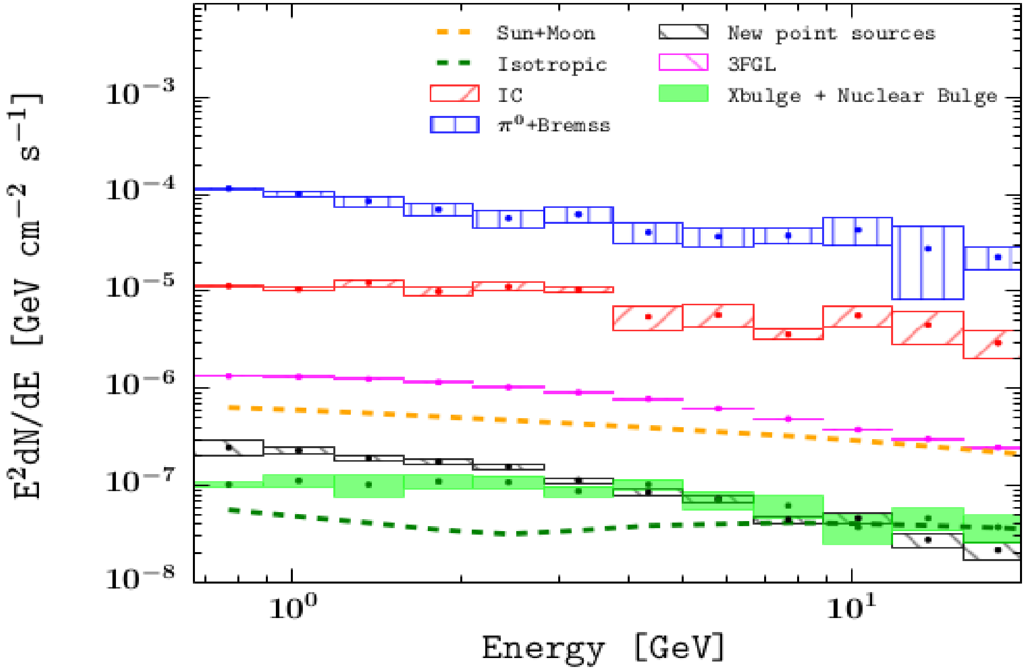


**Spectrum of model components is physically plausible.**

# Fermi Bubbles Vs X-shaped bulge

*Ness & Lang (2016),*
*Macias et al. (2016)*

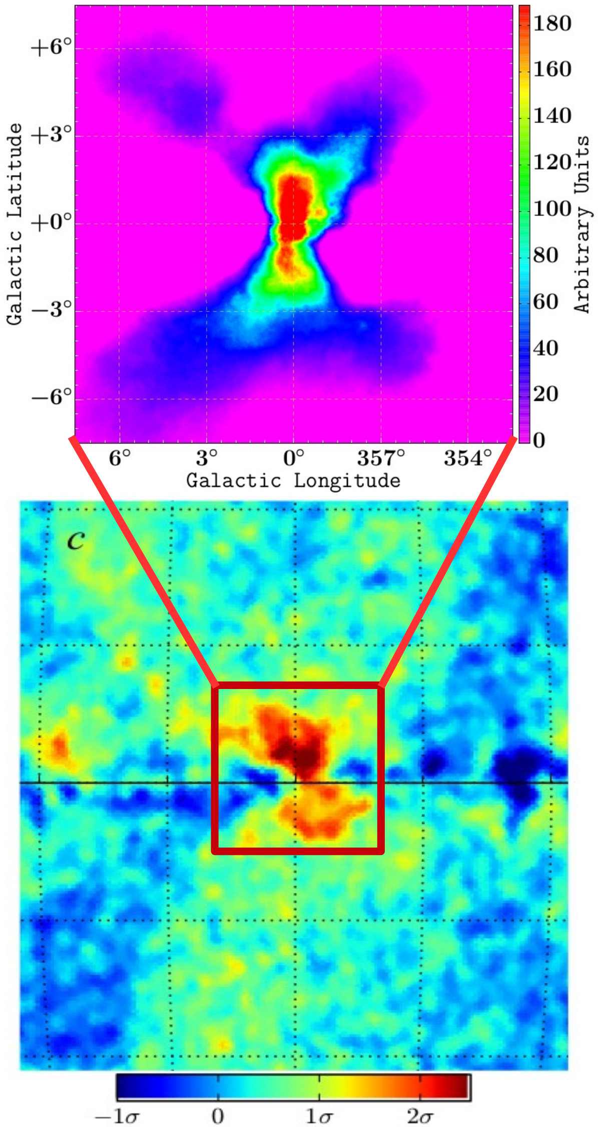


ApJ.Suppl. 223 (2016) no.2, 26

- **Recent work by the Fermi collaboration arguably shows a similar X-shaped excess at the base of the Fermi bubbles.**

- **However, our analysis shows distinct spectral characteristics to the overall Fermi bubbles ones: while the bubbles are described by** $\propto E^{-1.9}$ **the Xbulge is by** $\propto E^{-2.34\pm0.05}$**.**

- **The luminosity per solid angle of the X-bulge is** $(2.7 \pm 0.3) \times 10^{38}$ erg/s/sr **while that of the Fermi bubbles corresponds to** $(6.3 \pm 0.1) \times 10^{37}$ erg/s/sr

- **When our analysis considers the Fermi bubbles template proposed by ApJSup 223(2016)no.2,26 we find it has a negligible TS-value.**

# Morphology of the Galactic Center excess in Ackermann et al. (2017)

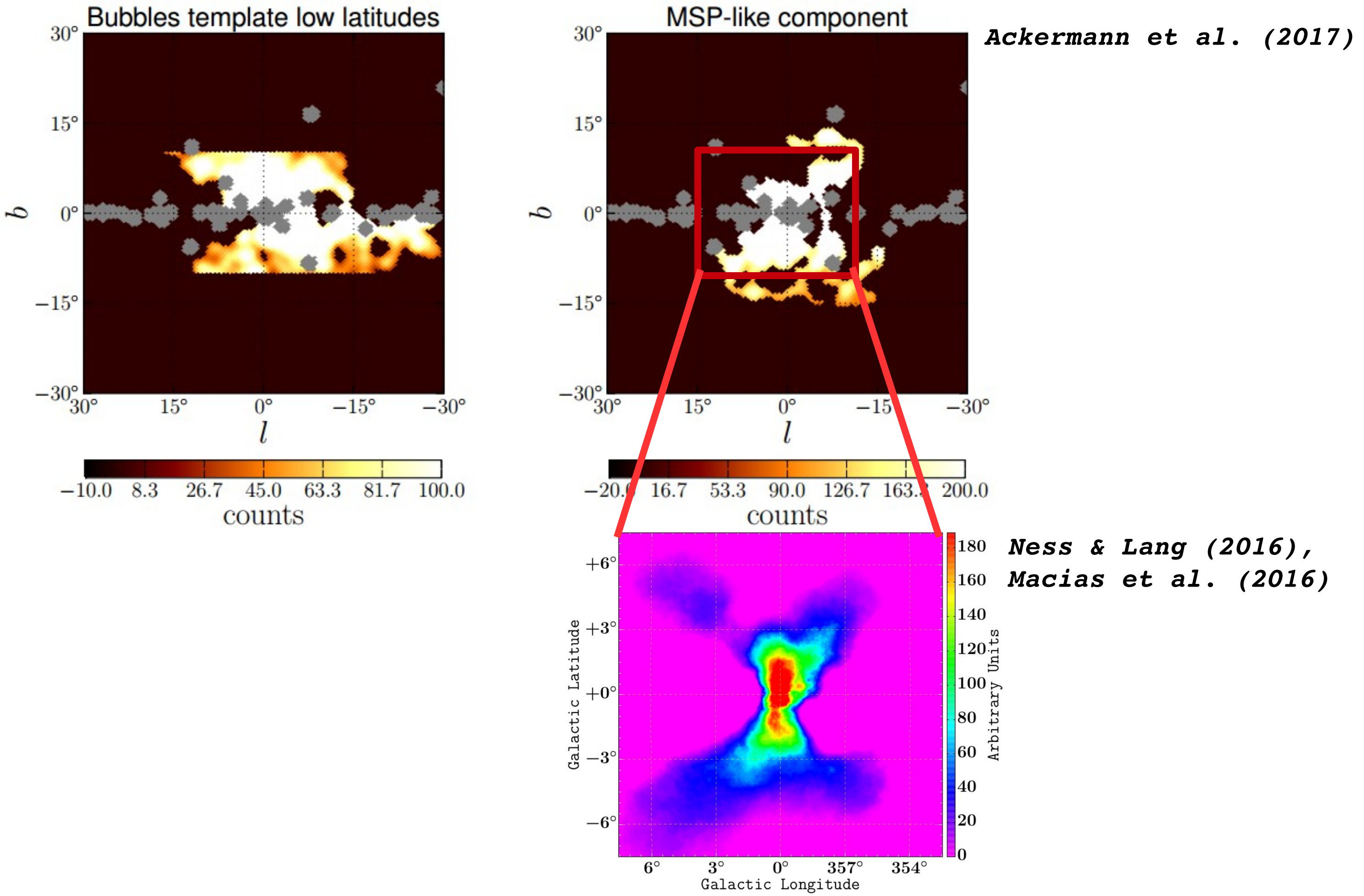


**MSPs-like component is concentrated in the inner 15x15 degrees and is not spherically symmetric**

# An unresolved population of Millisecond pulsars traced by the X-shaped and Nuclear Bulge could explain the Fermi GeV excess

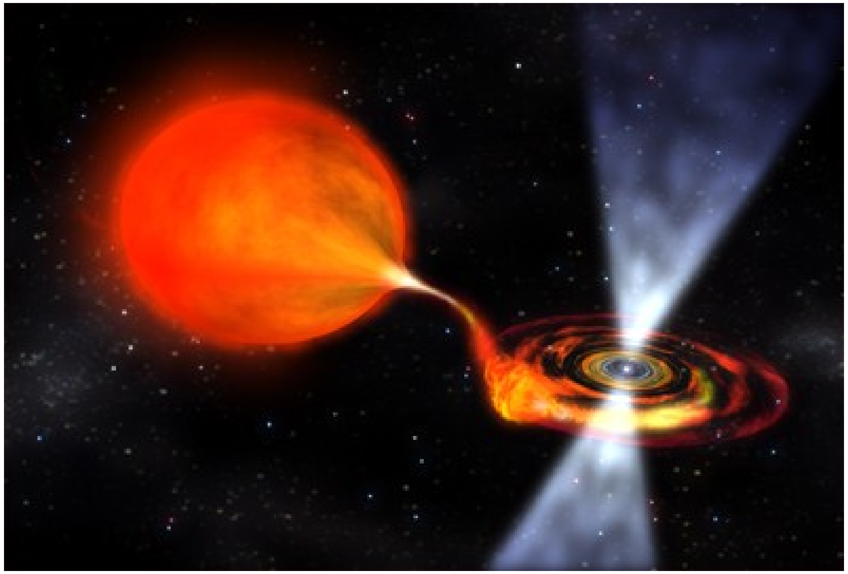

Image Credit: NASA/Dana Berry.

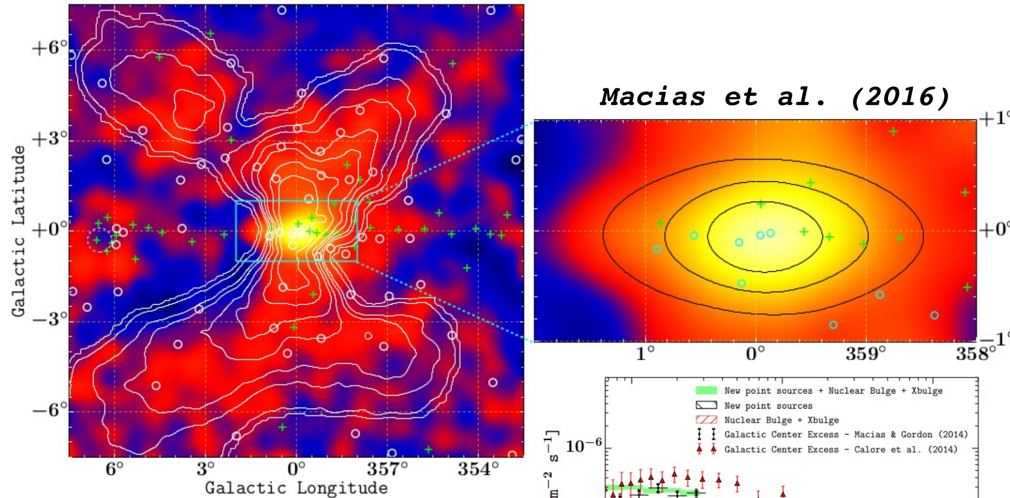


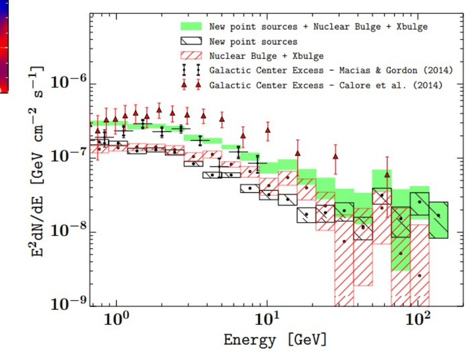


- The stellar mass of the X-bulge plus the nuclear bulge is $\sim 2.9 \times 10^9\ M_\odot$ therefore the Luminosity-to-Mass ratio for E>100 MeV is $\sim 3 \times 10^{27}\ \mathrm{erg/s}/M_\odot$ . From Winter et al. (2016) we infer the total MSPs luminosity of the Galaxy to be $\sim 2 \times 10^{27}\ \mathrm{erg/s}/M_\odot$ while for 47 Tuc is $\sim 5 \times 10^{28}\ \mathrm{erg/s}/M_\odot$.

# An unresolved population of Millisecond pulsars traced by the X-shaped and Nuclear Bulge could explain the Fermi GeV excess

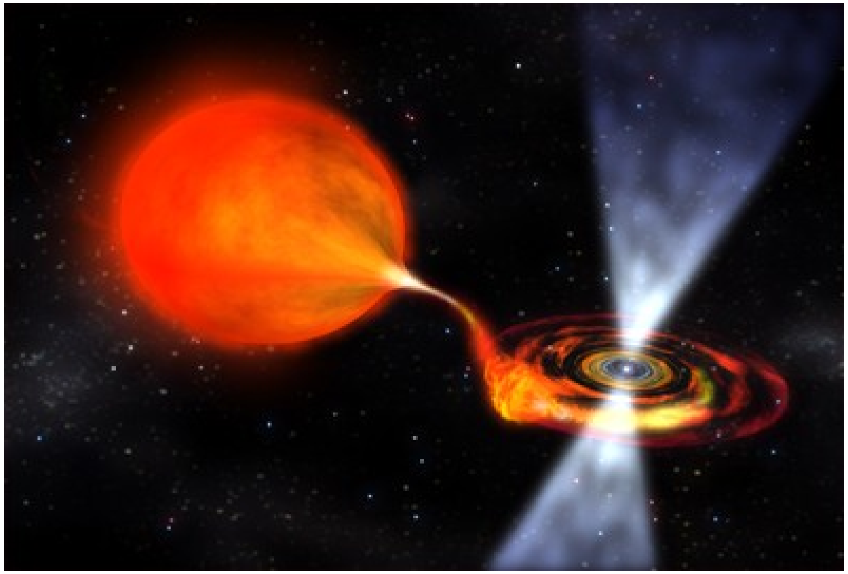

*Image Credit: NASA/Dana Berry.*

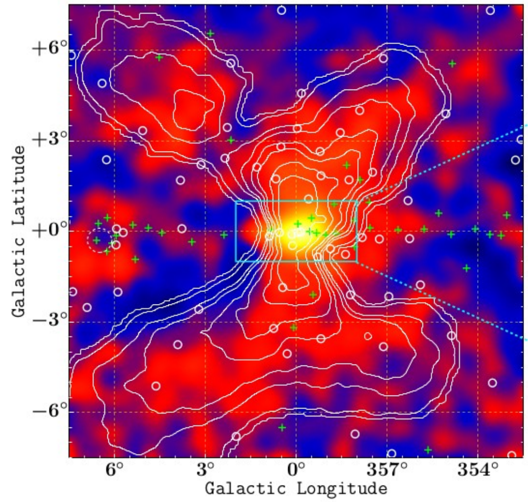


**Macias et al. (2016)**

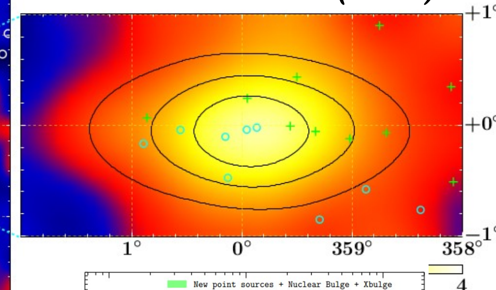

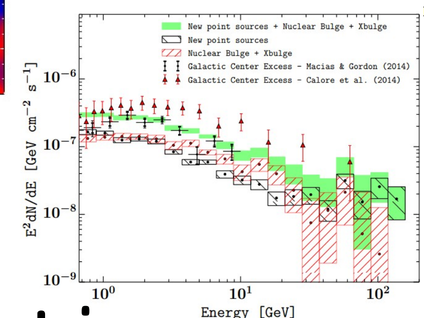


**Luminosity-to-mass ratio**

**Entire Galaxy** → $\sim 2 \times 10^{27}\ \mathrm{erg/s}/M_\odot$

**X-shaped bulge** → $\sim 3 \times 10^{27}\ \mathrm{erg/s}/M_\odot$

**47 Tuc** → $\sim 5 \times 10^{28}\ \mathrm{erg/s}/M_\odot$

# Pulsar detection sensitivity (gamma-rays)

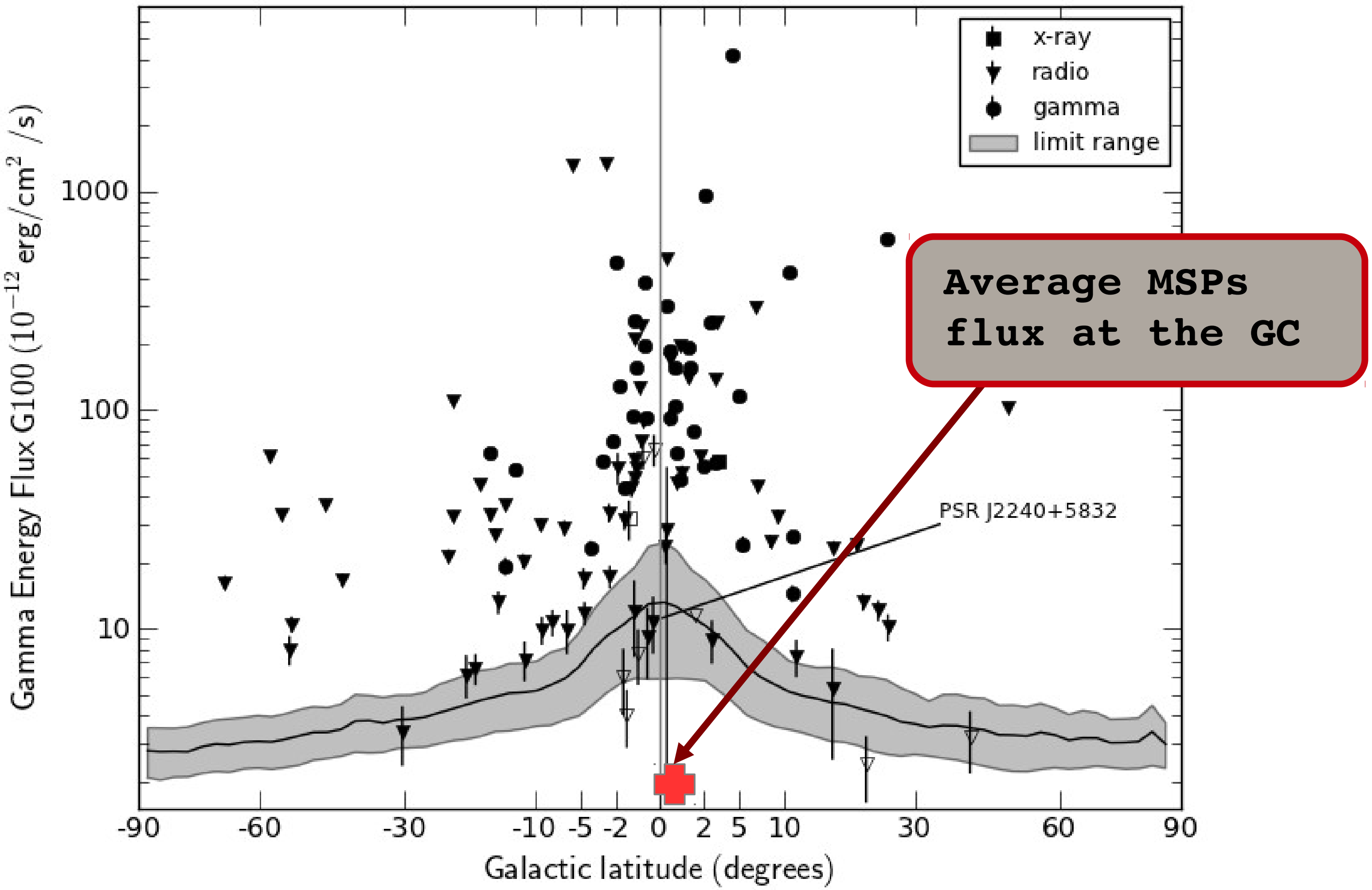


Credit: Fermi-LAT collaboration ApJ 208, 17 (2013)

# Pulsar detection sensitivity (Radio band)

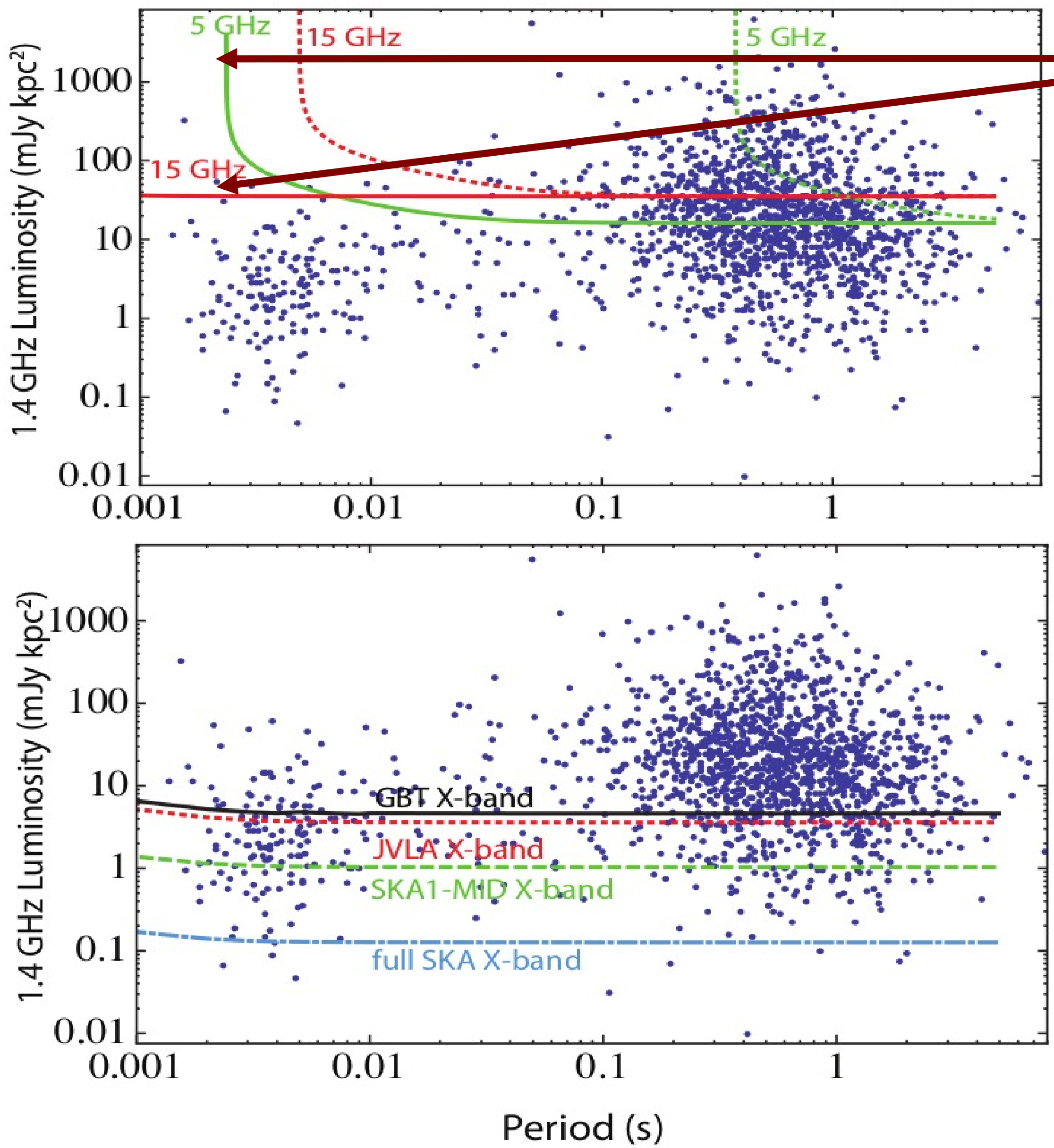


$10\sigma$ sensitivities of previous 5 GHz and 15 GHz GBT searches at the GC

Deep X-band observations of GBT and VLA would be sensitive to a significant fraction of the known MSP population if located at the GC distance.

Macquart & Kanekar (2015)

# Interpolated vs Hydrodynamical method

***Macias et al. (2016)***

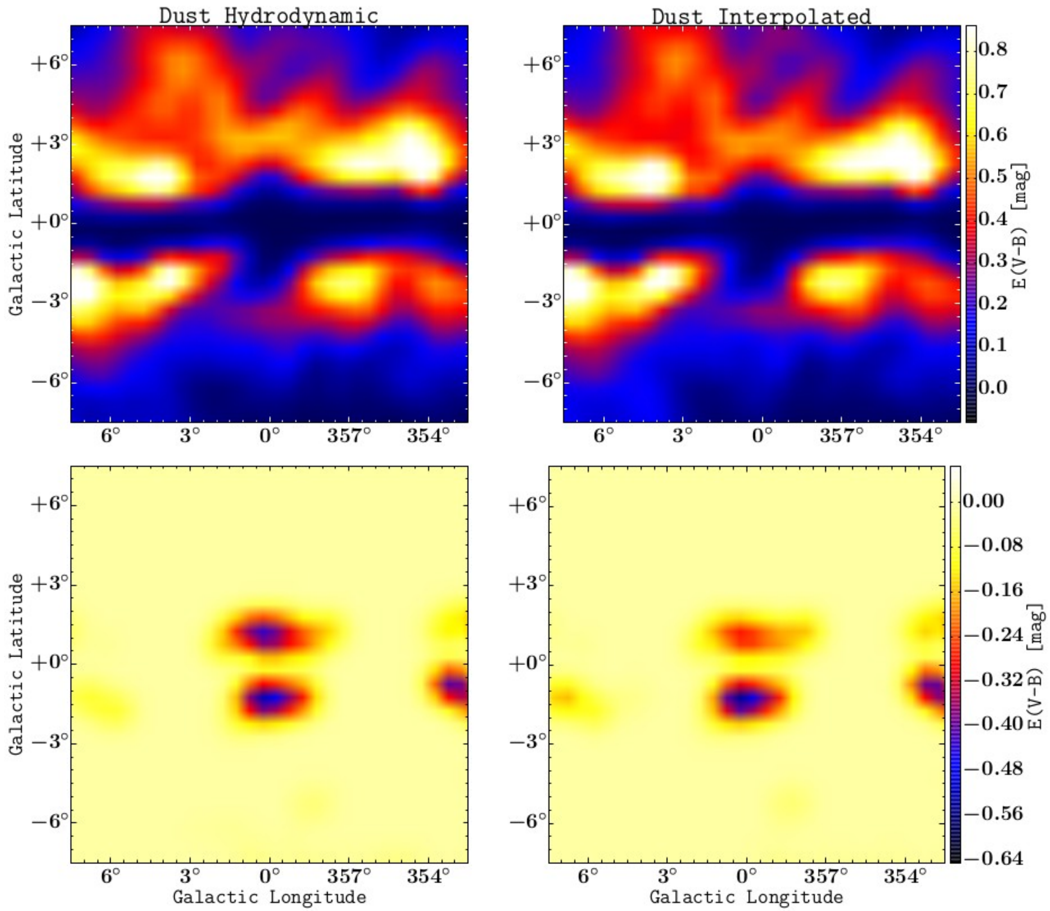


**Schelegel, Finkbeiner & Davis (1998)**

**Dust emission provides an alternative method of tracing hydrogen gas in the Galaxy.**

# Empirical maps accounting for observed residuals

Credit: Fermi-LAT collaboration ApJ.Suppl. 223 (2016) no.2, 26

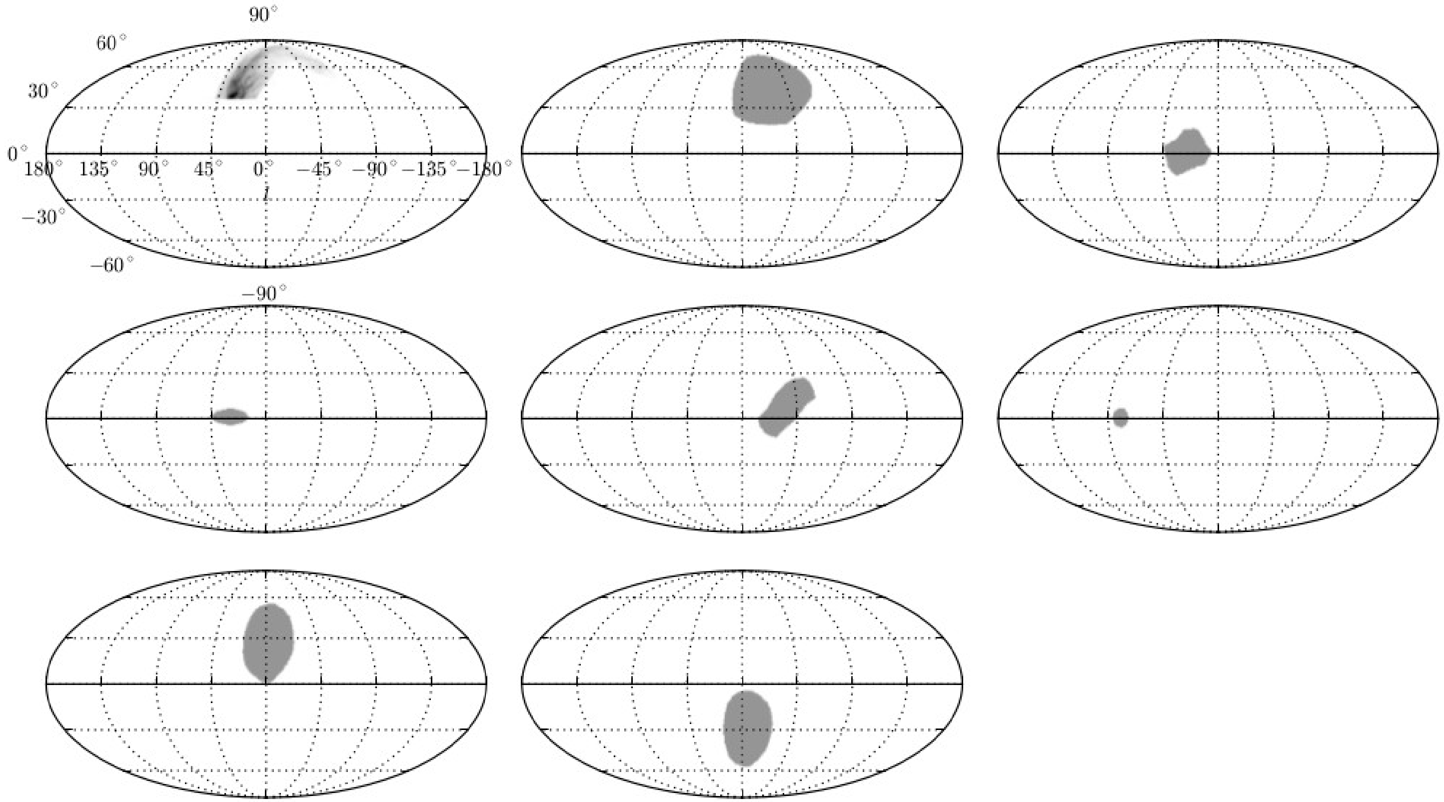


- The Fermi-LAT Galactic background model is only recommended for analyses of astrophysical compact objects.

# Dark Matter annihilations improve the fit only at the $1\sigma$ level

*Macias et al. (2016)*

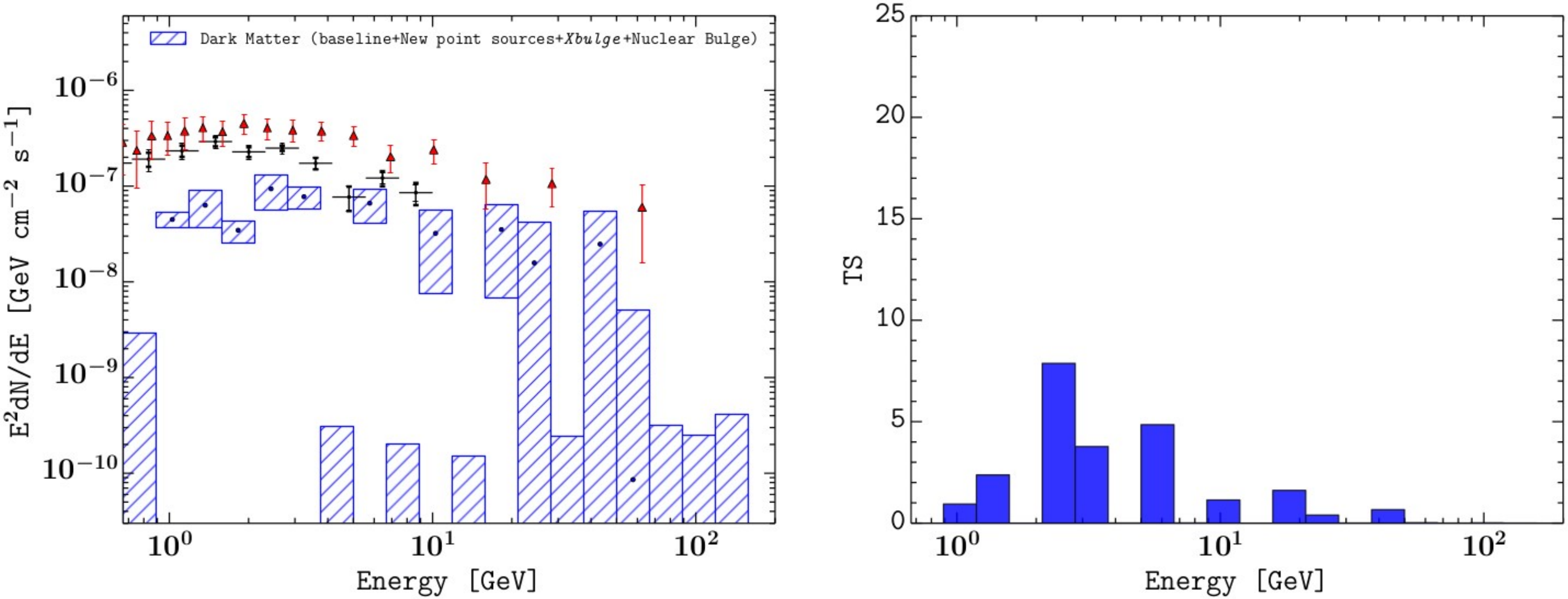


Dark matter is no longer favored by the data!

# There is a similar GC excess in Andromeda!

arXiv.org > astro-ph > arXiv:1702.08602

Astrophysics > High Energy Astrophysical Phenomena

## Observations of M31 and M33 with the Fermi Large Area Telescope: a galactic center excess in Andromeda?

Fermi-LAT Collaboration

(Submitted on 28 Feb 2017)

**Andromeda is ~770 kpc away**

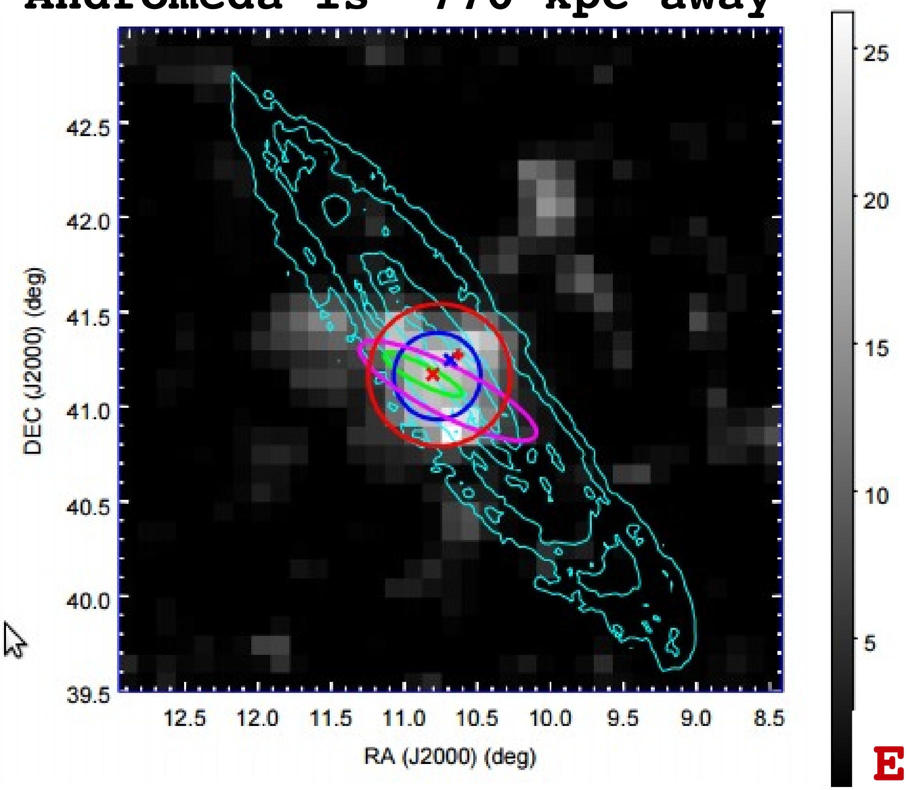


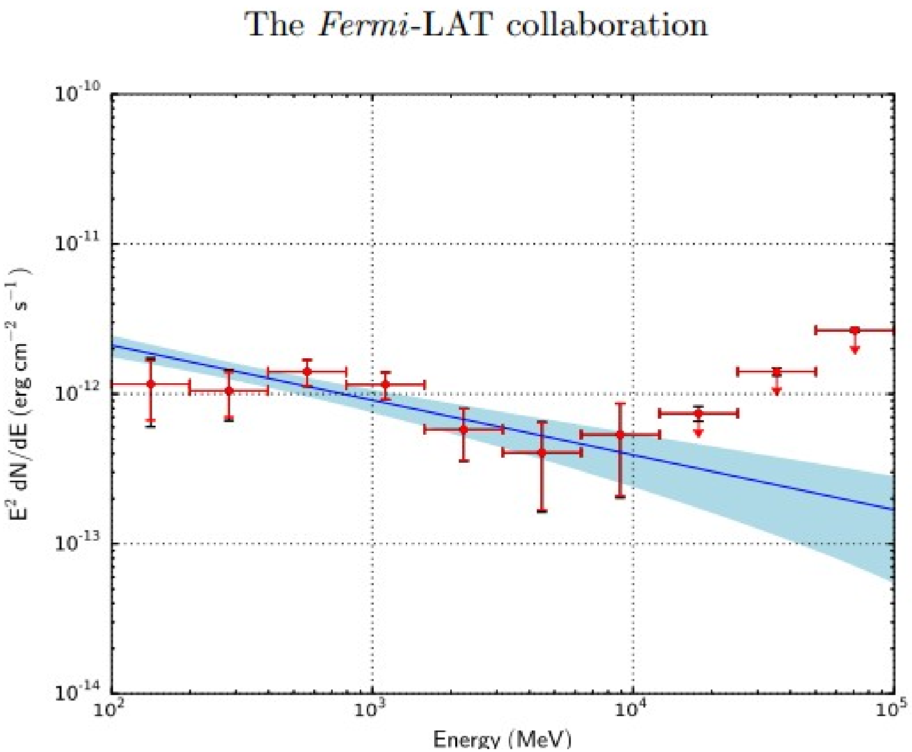


**Excess detected at ~10 \sigma**